

Lanthanide luminescent logic gate mimics in soft matter: [H⁺] and [F⁻] dual-input device in a polymer gel with potential for selective component release

Samuel J. Bradberry^{*a}, Joseph P. Byrne^a, Colin P. McCoy^b and
Thorfinnur Gunnlaugsson^{*a}

^a School of Chemistry and Trinity Biomedical Sciences Institute (TBSI), Trinity
College Dublin, 152 -160 Pearse Street, Dublin 2, Ireland

^{*}gunnlaut@tcd.ie; bradbers@tcd.ie

^b School of Pharmacy, Queen's University Belfast, Belfast, BT9 7Bl, United Kingdom

Electronic Supporting Information

General Experimental Details

Chemicals were purchased from commercial suppliers: Sigma-Aldrich Ireland Ltd., TCI Europe Ltd and Acros Organics and were used, unless stated, used without further purification. Synthesis was completed, unless stated, under inert atmospheres of N₂ or Ar. All microwave reactions were carried out in 2–5 mL or 10–20 mL Biotage Microwave Vials in a Biotage Initiator Eight EXP microwave reactor.

NMR solvents were purchased per-deuterated from Apollo Scientific. Silica chromatography was carried out on a Teledyne Isco CombiFlash automated machine using pre-packed RediSep® cartridges. Thin Layer Chromatography (TLC) was run using Merck Kiesegel 60 F₂₅₄ silica plates and visualised under UV irradiation ($\lambda = 254$ nm) and ethanolic ninhydrin staining. Melting points were determined using an Electrothermal IA900 digital apparatus. NMR was recorded using either an Agilent DD2/LH spectrometer, at 400.1 MHz and 100.6 MHz for ¹H and ¹³C experiments, respectively; or a Bruker AV-600 spectrometer at 600.1 MHz and 150.2 MHz for ¹H and ¹³C experiments, respectively.

Electrospray mass spectrometry was completed using a Mass Lynz NT V 3.4 on a Waters 600 controller with 996 photodiode array detector. HPLC grade solvents were used throughout and accurate molecular weights determined *via* a peak-matching method against enkephaline standard reference ($m/z = 556.2771$); all accurate masses were reported within ± 5 ppm of the calculated mass. Infrared spectra were recorded on a Perkin Elmer Spectrum One FT-IR spectrometer fitted with a universal ATR sampling accessory. Where applicable, elemental analysis (CHN) was carried out by the School of Chemistry, University College Dublin.

Photophysical and Spectroscopic Details

Unless otherwise stated, all measurements were performed at 298 K in CH₃OH solutions (spectroscopy grade, Aldrich). UV-visible absorption spectra were measured in 1-cm quartz cuvettes on a Varian Cary 50 spectrophotometer. Baseline correction was applied for all spectra. Emission (fluorescence, phosphorescence and excitation) spectra and lifetimes were recorded on a Varian Cary Eclipse Fluorimeter.

Gels were cut to 30 mm x 10 mm x 1.2 mm and suspended in a stirred CH₃OH solution and placed a 45° to the excitation light.

Phosphorescence lifetimes of the Eu(III) excited state were measured in both water/deuterated water or methanol/deuterated methanol solutions in time-resolved mode at 298 K. They are averages of three independent measurements, which were made by monitoring the emission decay at 616 nm, which corresponds to the maxima of the Eu(III) ⁵D₀→⁷F₂ transition, enforcing a 0.1 ms delay, and were analyzed using Origin 8.5®. The number of water molecules directly bounded to Eu(III) center (*q* value) was determined according to the equation developed by Parker *et al* [1]:

$$q = A(\tau_{O-H}^{-1} - \tau_{O-D}^{-1}) \quad (1),$$

where τ_{O-H} is the life-time water or methanol solutions, τ_{O-D} is the life-time measured in deuterated water or deuterated methanol solutions.

The quantum yields ($Q_{rel}^{Eu,L}$) were measured by relative method [2,3] using Cs₃[Ln(dpa)₃]·9H₂O complex in 0.1 M Tris buffer (pH = 7.45) ($Q_{abs}^{Eu} = 24.0 \pm 2.5 \%$) [4] as

a standard with known quantum yield, to which the absorbance and emission intensity of the sample are compared according to:

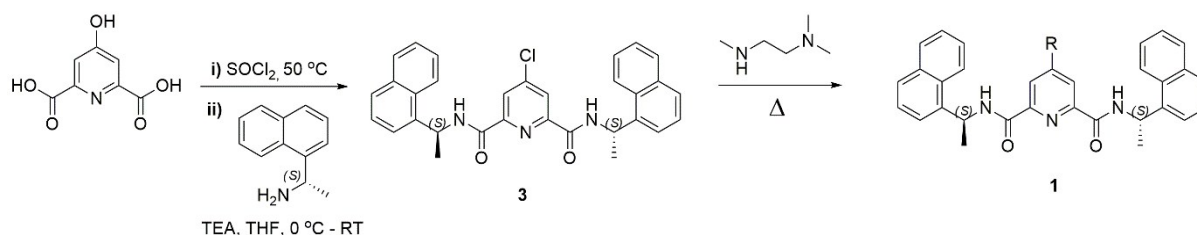
$$Q_{rel}^{Eu,L} = \frac{Q_x}{Q_r} = \frac{E_x}{E_r} \times \frac{A_r(\lambda_r)}{A_x(\lambda_x)} \times \frac{I_r(\lambda_r)}{I_x(\lambda_x)} \times \frac{n_x^2}{n_r^2} \quad (2)$$

where subscript r – reference and x – sample; E – integrated luminescence intensity; A – absorbance at the excitation wavelength; I – intensity of the excitation light at the same wavelength, n – refractive index of the solution. The estimated error for quantum yields is $\pm 10\%$.

References

- [1] A. Beeby, I.M. Clarkson, R.S. Dickins, S. Faulkner, D. Parker, L. Royle, A.S. de Sousa, J.A.G. Williams, M. Woods, *J. Chem. Soc., Perkin Trans. 2* **1999**, 493-503.
- [2] G.F. de Sá, L. Nunez, Z.M. Wang, G.R. Choppin, *J. Alloys Comp.* **1993**, 196, 17-23.
- [3] J.N. Demas, G.A. Crosby, *J. Phys. Chem.* **1971**, 75, 991-1024.

Synthesis



4-Chloro-*N,N'*-bis(1-(naphthalen-1-yl)ethyl)pyridine-2,6-dicarboxamide (3)

Chelidamic acid monohydrate was heated (0.40 g, 1.99 mmol) in SOCl_2 (5 mL) with cat. DMF (3 drops) at $50\text{ }^\circ\text{C}$ for 18 hours until complete dissolution. Excess SOCl_2 was distilled under reduced pressure. The residue dried under high vacuum then dissolved into THF (50 mL) and treated with (S) -1-(1-naphthyl)ethylamine (0.64 mL, 3.99 mmol) and TEA (0.56 mL, 3.99 mmol) at $0\text{ }^\circ\text{C}$.

After 30 minutes the reaction was allowed to warm to RT and stirred for 48 hours. Solvent was removed *in vacuo* then residues redissolved into CH_2Cl_2 (150 mL). This solution was washed with sat. aq. NaHCO_3 (2 x 50 mL), brine (50 mL) and the organic phase dried over MgSO_4 , filtered and concentrated *in vacuo*. Trituration under CH_3OH and filtration of resultant solids yielded **20S** as a white solid (0.615 g, 1.21 mmol, 61%); m.p. $129.9 - 131.2\text{ }^\circ\text{C}$; HRMS (m/z) (ES^+) Calculated for $\text{C}_{31}\text{H}_{27}\text{ClN}_3\text{O}_2$ $m/z = 508.1766$ [$\text{M} + \text{H}$] $^+$. Found $m/z = 507.1714$; ^1H NMR (400 MHz, CDCl_3) δ : 8.34 (2H, s, **10**), 8.13 (2H, br. d, $J = 5.9$ Hz, naph-CH), 7.85 (2H, br. d, $J = 7.5$ Hz, naph-CH), 7.63 (2H, d, $J = 7.7$ Hz, naph-CH), 7.55 – 7.49 (4H, m, naph-CH), 7.49 – 7.39 (4H, m, naph-CH), 6.12 – 5.89 (2H, m, **8**), 1.67 (6H, d, $J = 6.6$ Hz, **9**). ^{13}C NMR (100 MHz, CDCl_3) δ : 161.34, 150.02, 147.70, 137.77, 133.92, 130.87, 128.94, 128.55, 126.68, 125.97, 125.52, 125.21, 123.13, 122.69, 45.40, 20.84; IR ν_{max} (cm^{-1}): 3281, 2976, 1644, 1599, 1510, 1373, 1334, 1232, 1173, 1118, 1081, 998, 900, 860, 800, 777, 765, 681.

4-((2-(Dimethylamino)ethyl)(methyl)amino)-N,N-bis(1-(naphthalen-1-yl)ethyl)pyridine-2,6-dicarboxamide (1)

Compound **3** (1 equiv.) was refluxed in distilled *N',N,N*-trimethylethylenediamine (1.5 mL) for 18 hours. Upon completion, by TLC, the reaction mixture was poured into iced-water (3 mL) precipitating beige solids which were isolated by filtration and washed with excess H₂O then dried *in vacuo*. Crude mixtures were eluted on silica (RediSep® 40g, 10 CV DCM) followed by gradient elution 0 → 15 % CH₃OH in DCM), product containing fractions were concentrated to give pure products as white solid. Yield: 63 %; m.p. 169.2 – 169.9 oC; HRMS (m/z) (ES⁺) Calculated for C₃₆H₄₀N₅O₂ m/z = 574.3182 [M + H]⁺. Found m/z = 574.3177; ¹H NMR (400 MHz, CDCl₃+0.1% NaOD) δ : 8.19 – 8.10 (2H, m, naph-CH), 7.95 – 7.86 (4H, m, naph-CH + 10), 7.86 – 7.79 (2H, m, naph-CH), 7.51 (5H, m, naph-CH), 7.47 – 7.37 (3H, m, naph-CH), 6.08 – 5.82 (2H, m, 8), 3.71 (2H, app. br. s, 11), 3.14 (3H, s, 14), 2.68 (2H, app. br. s, 12), 2.44 (6H, s, 13) 1.65 (6H, d, J = 6.8 Hz, 9). ¹³C NMR (100 MHz, CDCl₃) δ : 163.35, 155.42, 146.73, 138.43, 133.97, 130.94, 128.88, 128.33, 126.52, 125.84, 125.29, 123.30, 122.63, 113.47, 109.94, 106.80, 45.23, 38.38, 30.90, 21.12. IR ν_{max} (cm⁻¹): 3300, 2977, 2824, 2769, 1654, 1604, 1517, 1453, 1396, 1775, 1145, 1020, 866, 802, 776.

2,6-Bis(1-(4-(carboxy)benzyl)-1,2,3-triazol-4-yl)pyridine (2) [4]

To a solution of 4-(bromomethyl) benzoic acid (4.65 mmol) in 15 mL DMF/water (4:1) was added sodium azide (0.332 g, 4.65 mmol) and the reaction mixture stirred for 1 hour, yielding the azide derivative, which was not isolated, and therefore used without further purification.

To this solution was added 2,6-bis(trimethylsilylethynyl)pyridine (0.631 g, 2.33 mmol). CuSO₄·5H₂O (0.232 g, 0.93 mmol) and sodium ascorbate (0.368 g, 1.86 mmol) were added to the reaction mixture, followed by anhydrous K₂CO₃ (0.650 g, 4.70 mmol) and stirred at room

temperature for 18 hours in a further 15 mL 4:1 DMF/water. EDTA/NH₄OH solution was added to the reaction mixture and stirred for 1 hour before isolating the product.

The product was isolated upon acidification of the EDTA/NH₄OH solution by dropwise addition of concentrated HCl solution until pH 7 was reached. **2** was collected as a beige solid upon suction filtration (0.705 g, 1.46 mmol, 63%). Product decomposed over 284 °C. HRMS (m/z) (ESI⁻): Calculated for C₂₅H₁₈N₇O₄⁻ m/z = 480.1426 [M-H]⁻. Found m/z = 480.1423; Calculated for C₂₅H₁₉N₇O₄·0.5H₂O, C = 57.46, H = 3.86, N = 18.76. Found C = 57.39, H = 3.75, N = 18.92. ¹H NMR (600 MHz, DMSO-*d*₆): δ (ppm) = 5.80 (s, 4H, CH₂), 7.45 (d, 4H, J = 8.7 Hz, Ph CH), 7.91–8.03 (m, 7H, Ph CH and pyr CH), 8.74 (s, 2H, triazolyl CH); ¹³C NMR (150 MHz, DMSO-*d*₆): δ (ppm) = 52.8 (CH₂), 118.7 (3- and 5-pyr CH), 124.1 (triazolyl CH), 128.2 (phenyl CH), 129.9 (Ph CH), 130.6 (Ph qt), 138.1 (4-pyr CH), 140.8 (Ph qt), 147.5 (triazolyl qt), 149.8 (2- and 4-pyr qt), 167.03 (C=O); IR ν_{max} (cm⁻¹): 3083 (ar C–H st), 2938 (C–H st), 1719, 1692 (C=O st), 1642, 1614, 1531, 1467, 1420, 1400, 1285, 1242, 1198, 1176, 1106, 1047, 942, 822, 800, 725.

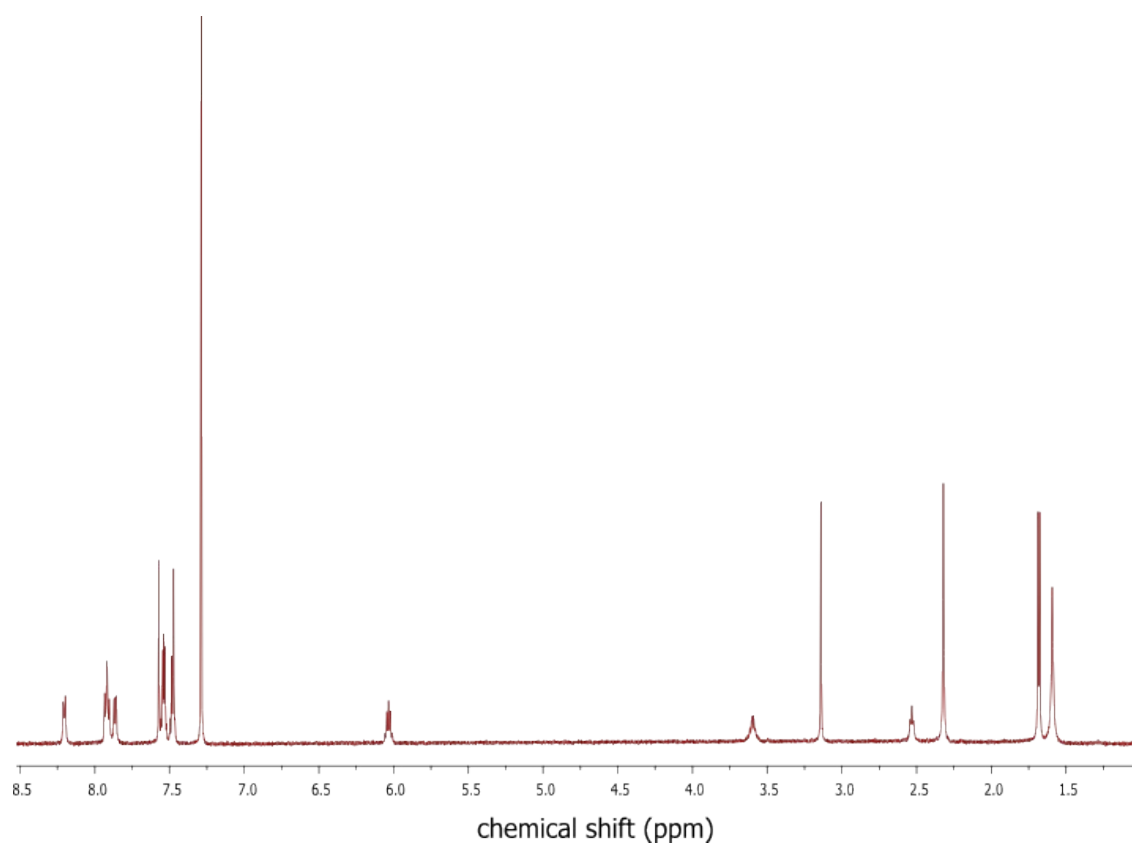
Complexation – **Eu.1₃** and **Tb.2₃**

Ligands **1** and **2** were dissolved in CH₃OH (5 mL) and treated with 0.33 equivalents Eu(CF₃SO₃)₃ and Tb(CF₃SO₃)₃, respectively, for 30 minutes at 70 °C. The resulting solutions were concentrated *in vacuo* then re-dissolved into minimal CH₃OH. The concentrated solutions were subsequently precipitated in rapidly stirred diethyl ether (100 ml) to give white (**Eu.1₃**) and brown (**Tb.2₃**) solids in 70% yields. Precipitates were collected via centrifugation and dried prior to use.

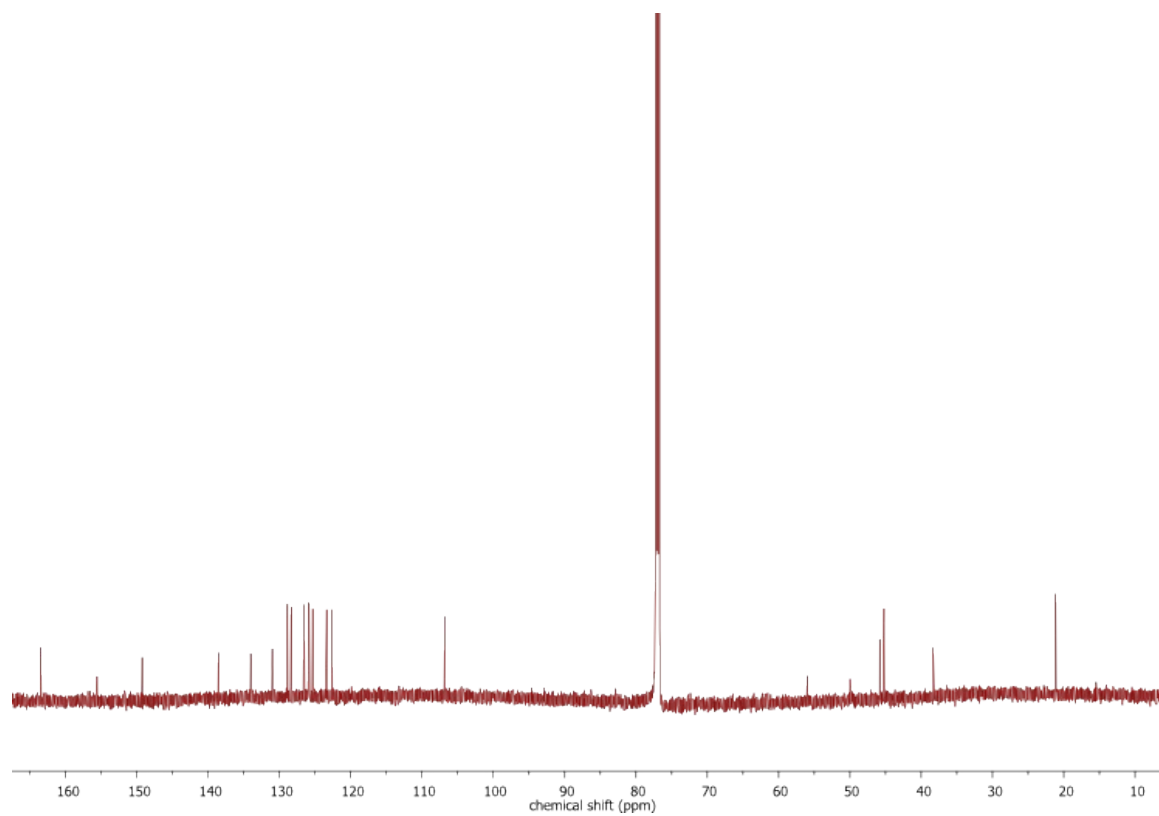
poly(HEMA-*co*-MMA) [5]

2-hydroxyethyl methacrylate (HEMA, 7.5 mL), methyl methacrylate (MMA, 2.5 mL) and ethylene glycol dimethacrylate (EGDMA, 0.1 mL) were stirred at RT. Complexes **Eu.1₃** (3 mg) and **Tb.2₃** (1 mg) were added in CH₃CN (200 μL) to stirred until dissolution had occurred. AIBN (100 mg) was added and the clear, homogenous solution injected into a non-stick mould and placed in a 90 °C oven for 6 hours. Then resulting acrylic materials were allowed to cool to RT, removed from the moulds and cut to the desired dimensions.

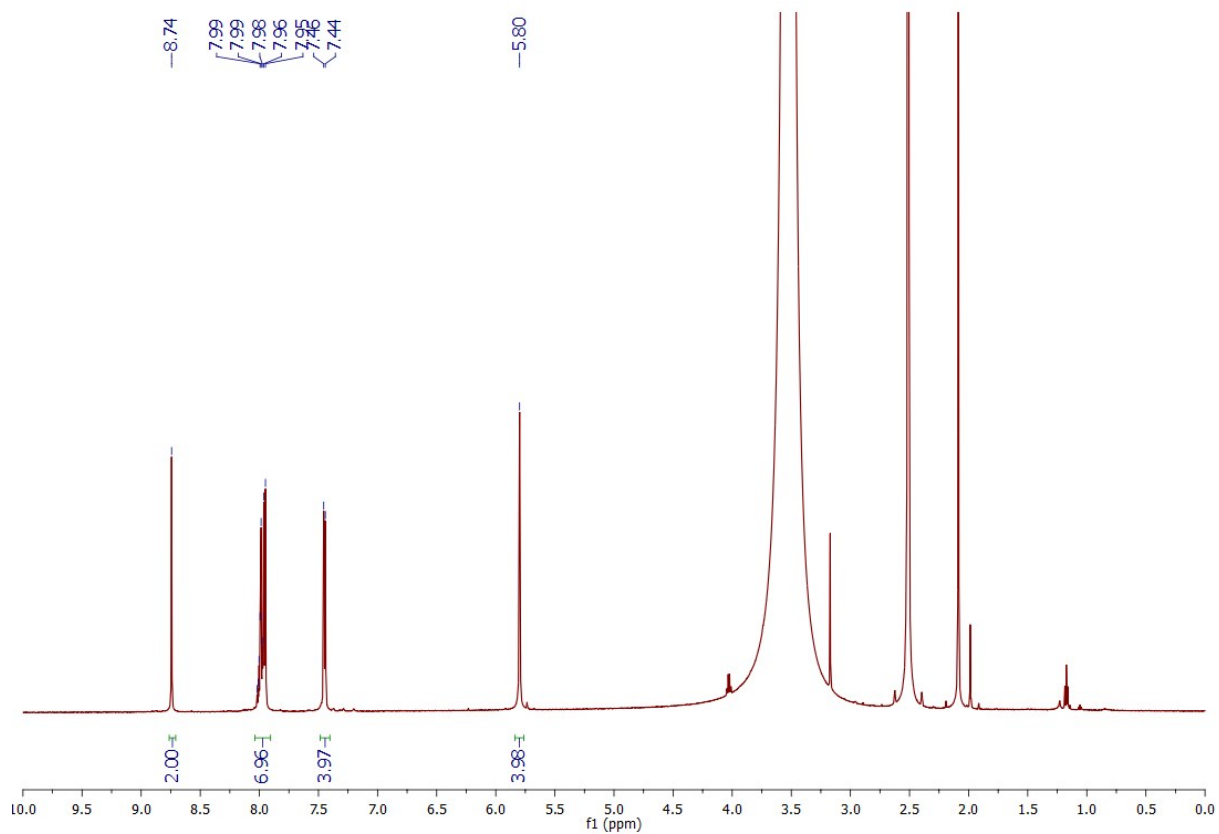
- [4] J. P. Byrne, J. A. Kitchen, J. E. O'Brien, R. D. Peacock and T. Gunnlaugsson, *Inorg. Chem.*, 2015, **54**, 1426-1439
- [5] C. P. McCoy, F. Stomeo, S. E. Plush and T. Gunnlaugsson, *Chem. Mater.*, 2006, **18**, 4336-4343



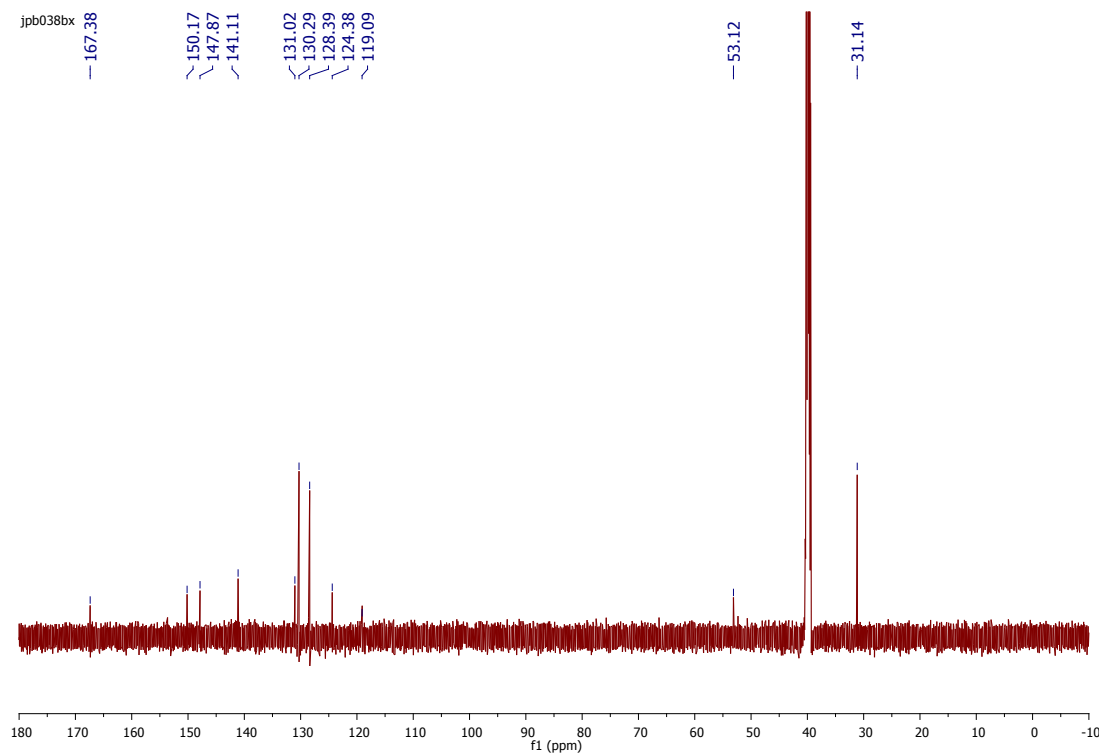
S1 ^1H NMR spectrum of **1** (600 MHz, CDCl_3)



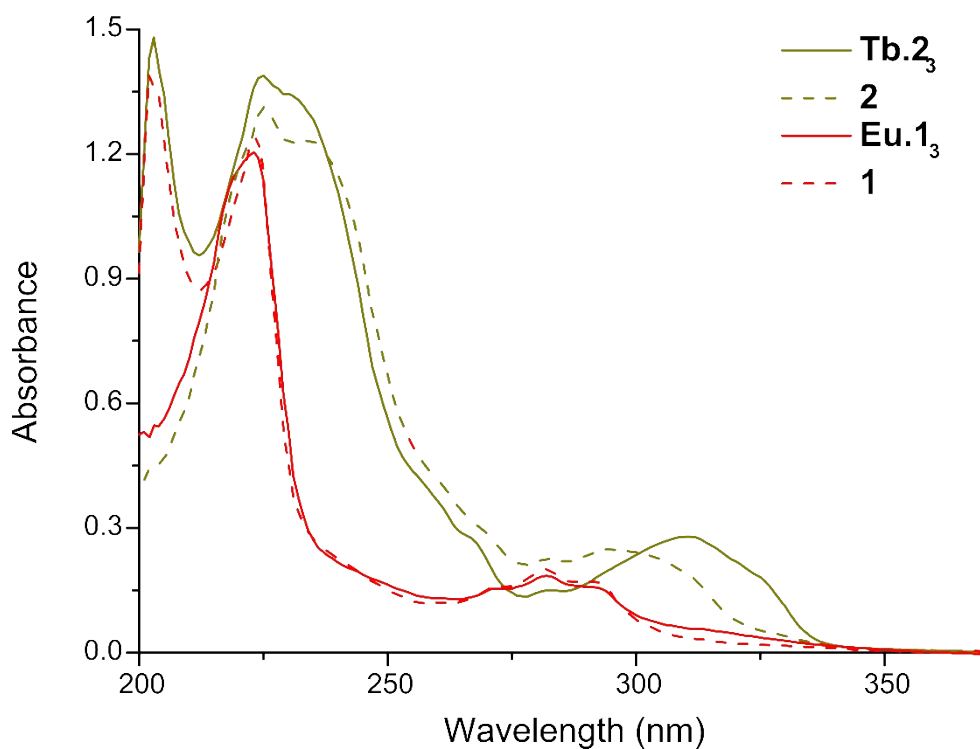
S2 ^{13}C NMR spectrum of **1** (150 MHz, CDCl_3)



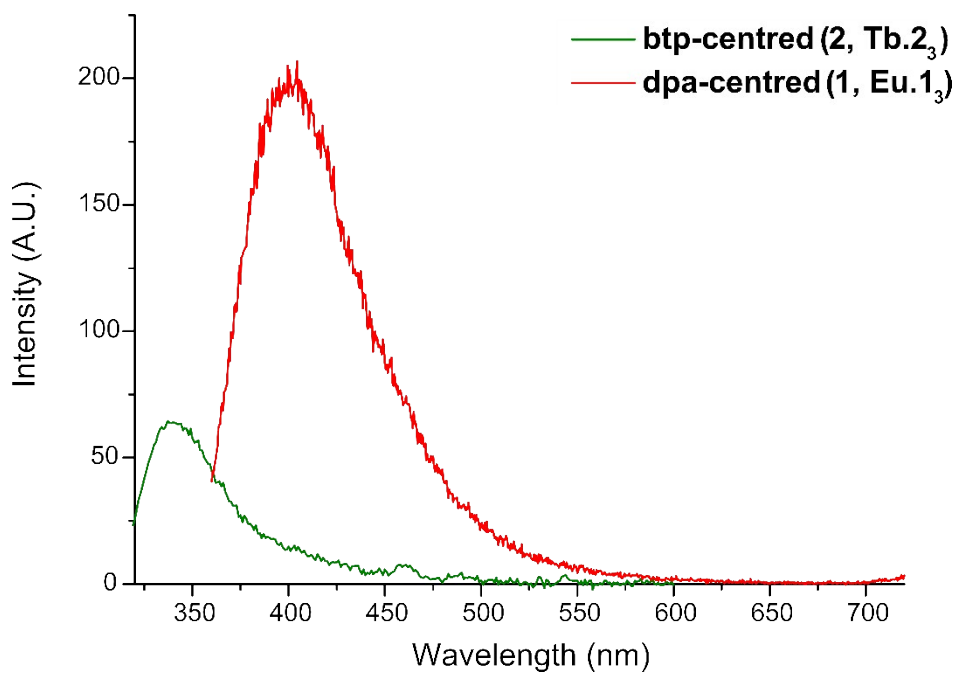
S3 ^1H NMR spectrum of **2** (600 MHz, DMSO- d_6)



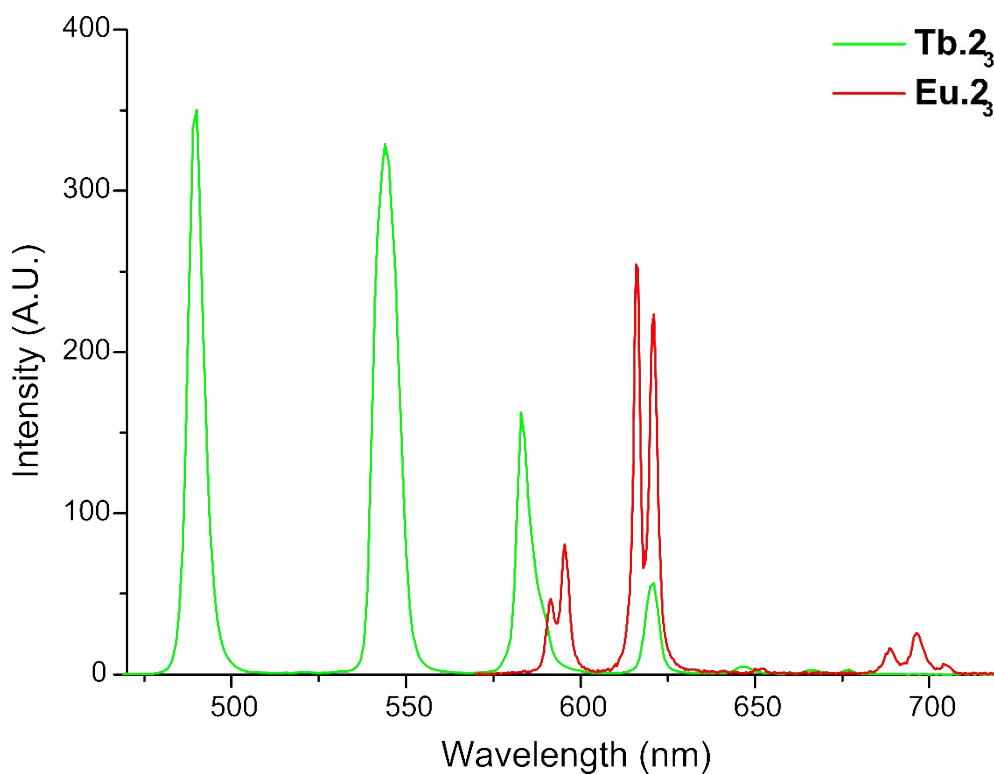
S4 ^{13}C NMR spectrum of **2** (150 MHz, DMSO- d_6)



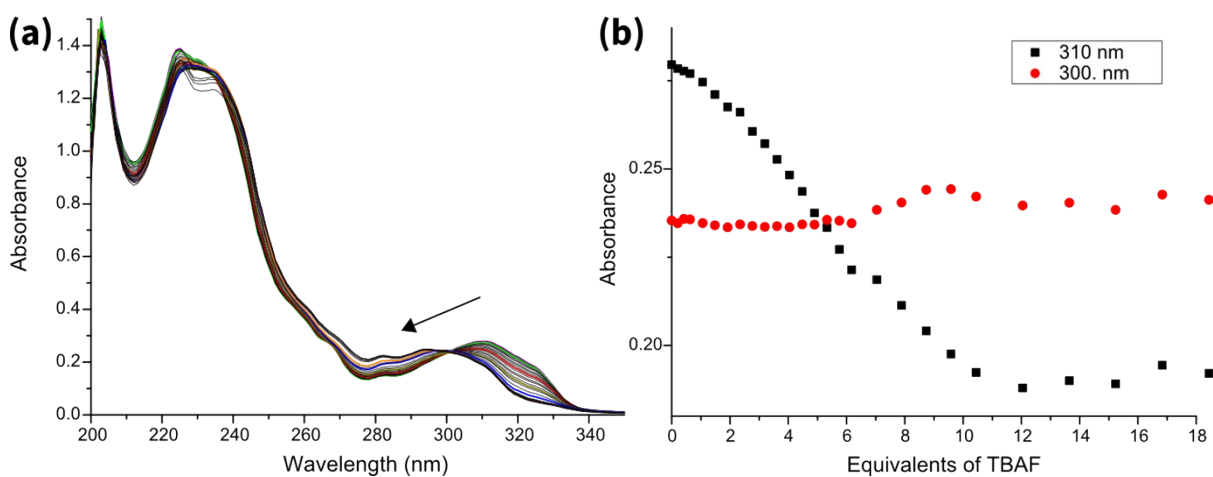
S5 Overlaid UV-Vis spectra of **1**, **2**, **Eu.1₃** and **Tb.2₃** at $c = 1 \times 10^{-5}$ M independently recorded in CH₃OH.



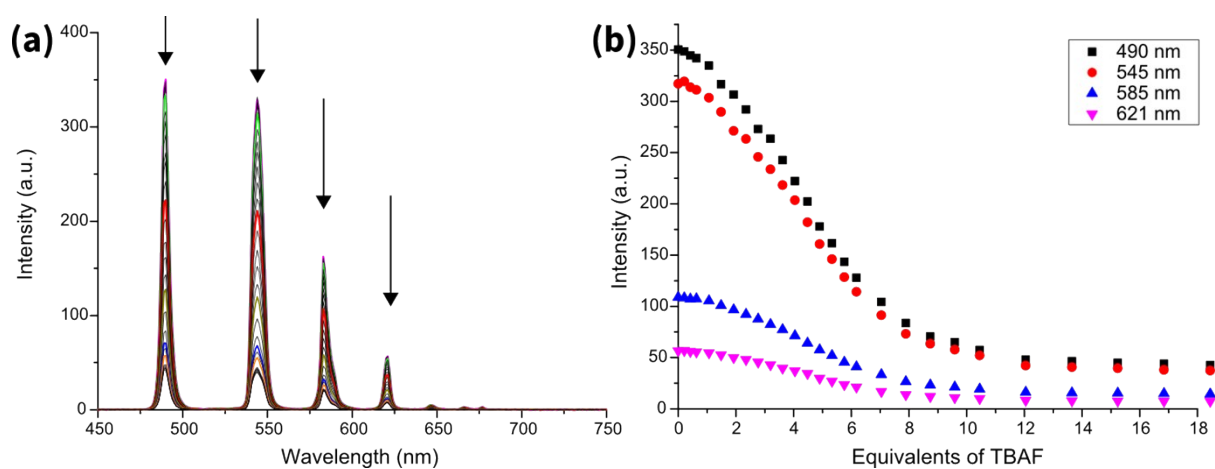
S6 Overlaid fluorescence spectra of **1**, **2** showing the ligand-centred fluorescence emissions, independently recorded in CH₃OH.



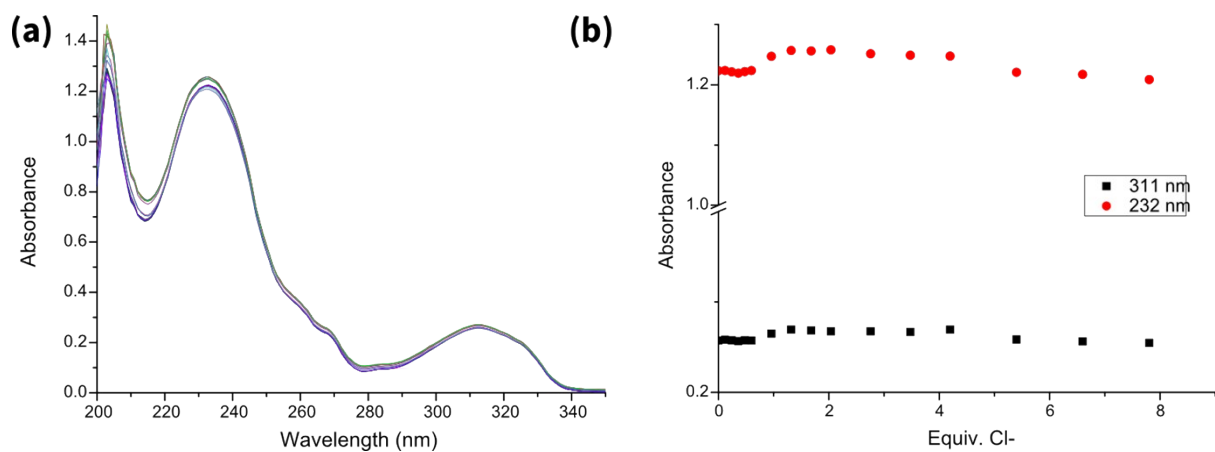
S7 Overlaid Phosphorescence spectra of **1**, **2**, **Eu.1₃** and **Tb.2₃** independently recorded in CH₃OH.



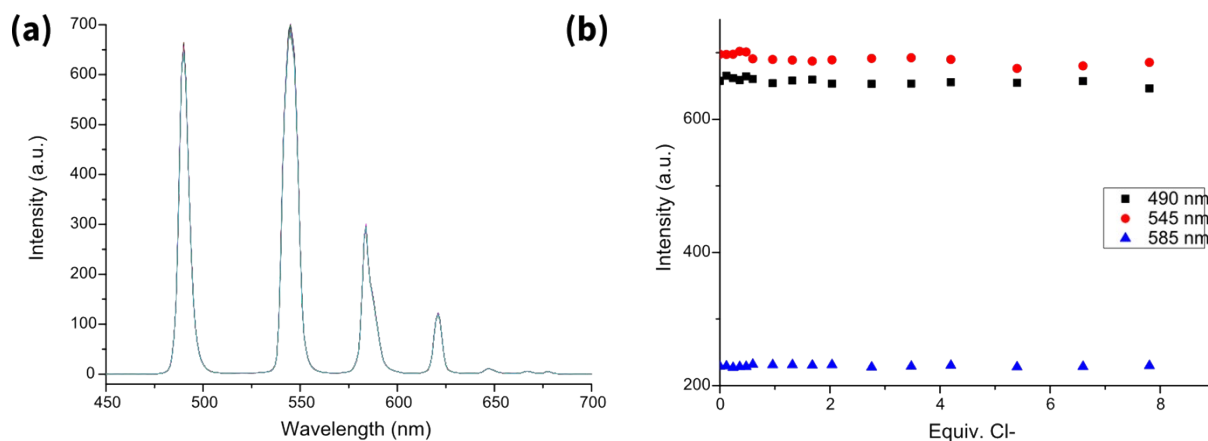
S8 (a) UV-Vis absorbance spectra upon addition of TBAF to a solution of **Tb.2₃** ($c = 1 \times 10^{-5}$ M) in CH₃OH **(b)** Absorbance changes at 300 and 310 nm plotted as a function of TBAF equivalents added.



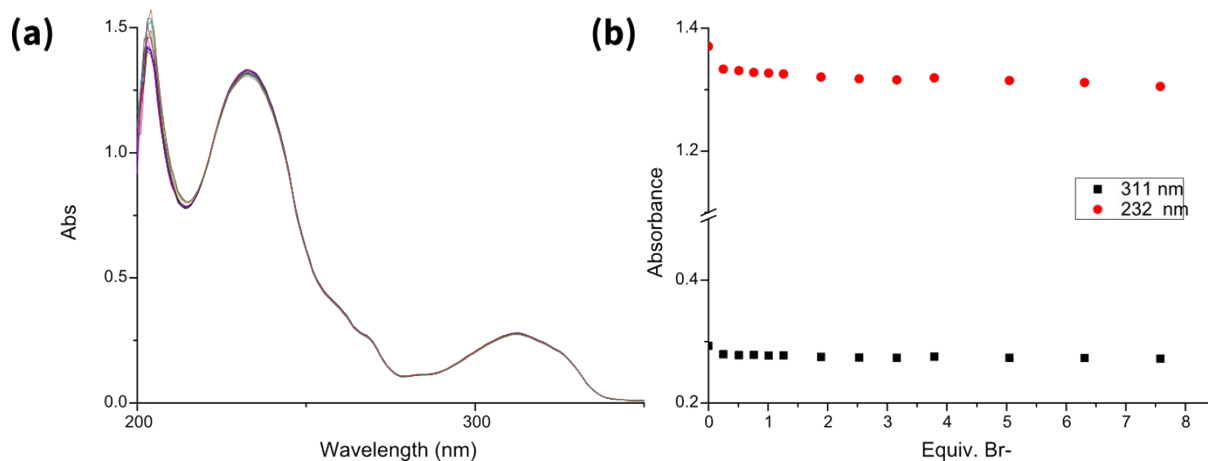
S9 (a) Phosphorescence spectra upon addition of TBAF to a solution of **Tb.2₃** ($c = 1 \times 10^{-5}$ M) in CH_3OH **(b)** Intensity changes in $^5\text{D}_4 \rightarrow ^7\text{F}_J$ transitions (490, 545, 585, 621 nm) plotted as a function of TBAF equivalents added.



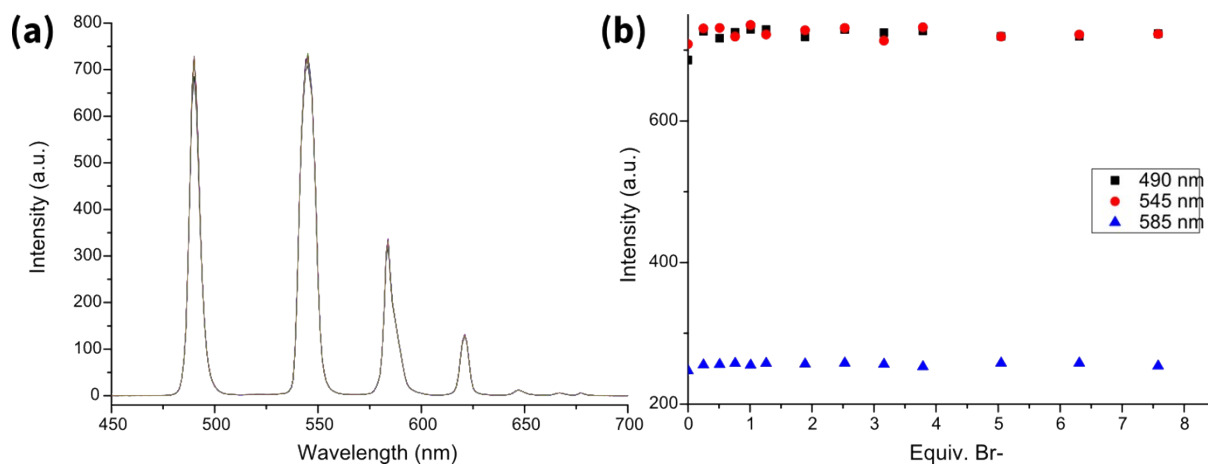
S10 (a) UV-Vis absorbance spectra upon addition of TBA-Cl to a solution of **Tb.2₃** ($c = 1 \times 10^{-5}$ M) in CH_3OH **(b)** Absorbance changes at 300 and 310 nm plotted as a function of TBA-Cl equivalents added.



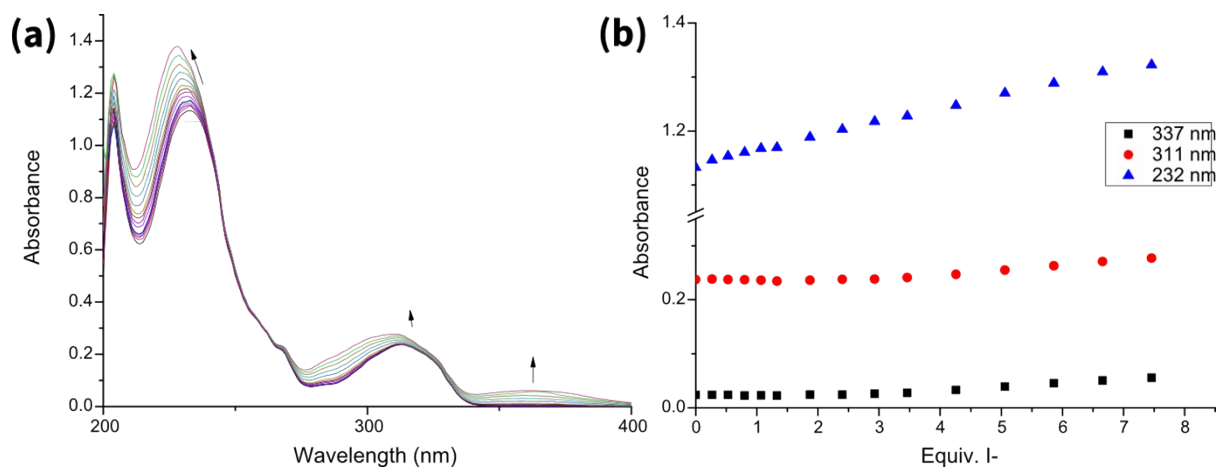
S11 (a) Phosphorescence spectra upon addition of TBACl to a solution of **Tb.2₃** ($c = 1 \times 10^{-5}$ M) in CH_3OH **(b)** Intensity changes in $^5\text{D}_4 \rightarrow ^7\text{F}_J$ transitions (490, 545, 585, 621 nm) plotted as a function of TBACl equivalents added.



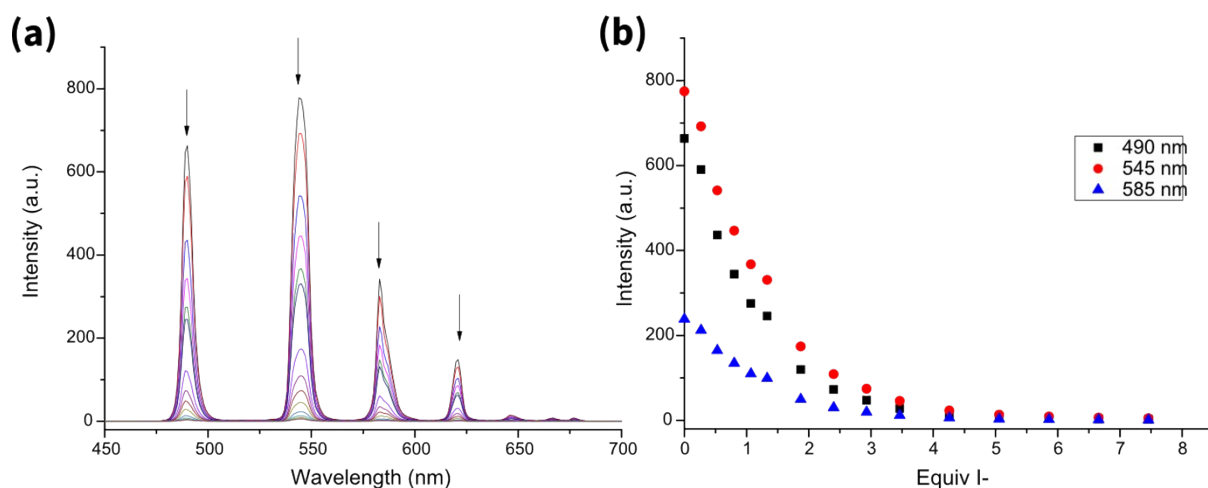
S12 (a) UV-Vis absorbance spectra upon addition of TBABr to a solution of **Tb.2₃** ($c = 1 \times 10^{-5}$ M) in CH_3OH **(b)** Absorbance changes at 300 and 310 nm plotted as a function of TBABr equivalents added.



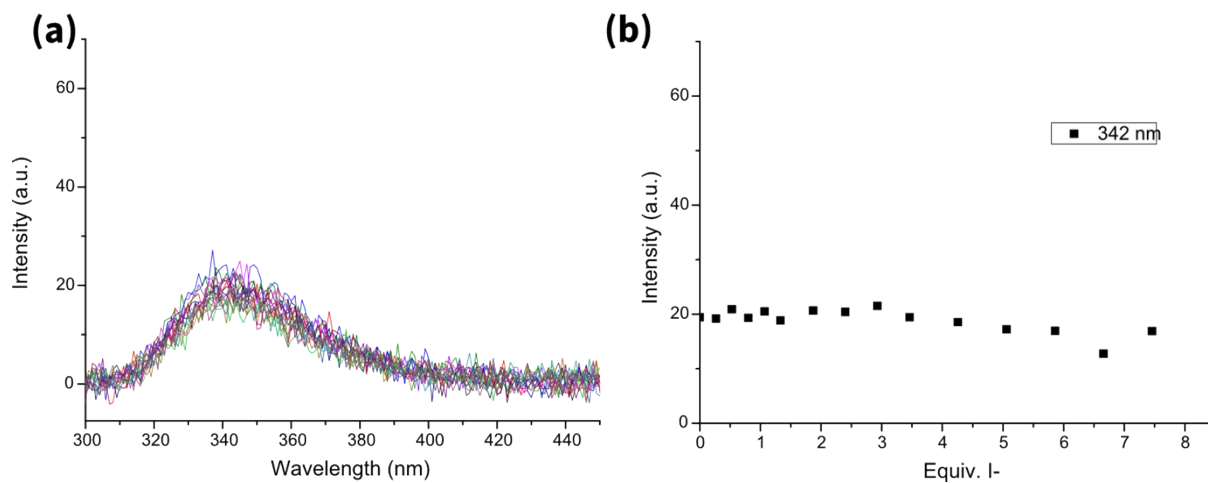
S13 (a) Phosphorescence spectra upon addition of TBABr to a solution of **Tb.2₃** ($c = 1 \times 10^{-5}$ M) in CH_3OH **(b)** Intensity changes in $^5\text{D}_4 \rightarrow ^7\text{F}_J$ transitions (490, 545, 585, 621 nm) plotted as a function of TBABr equivalents added.



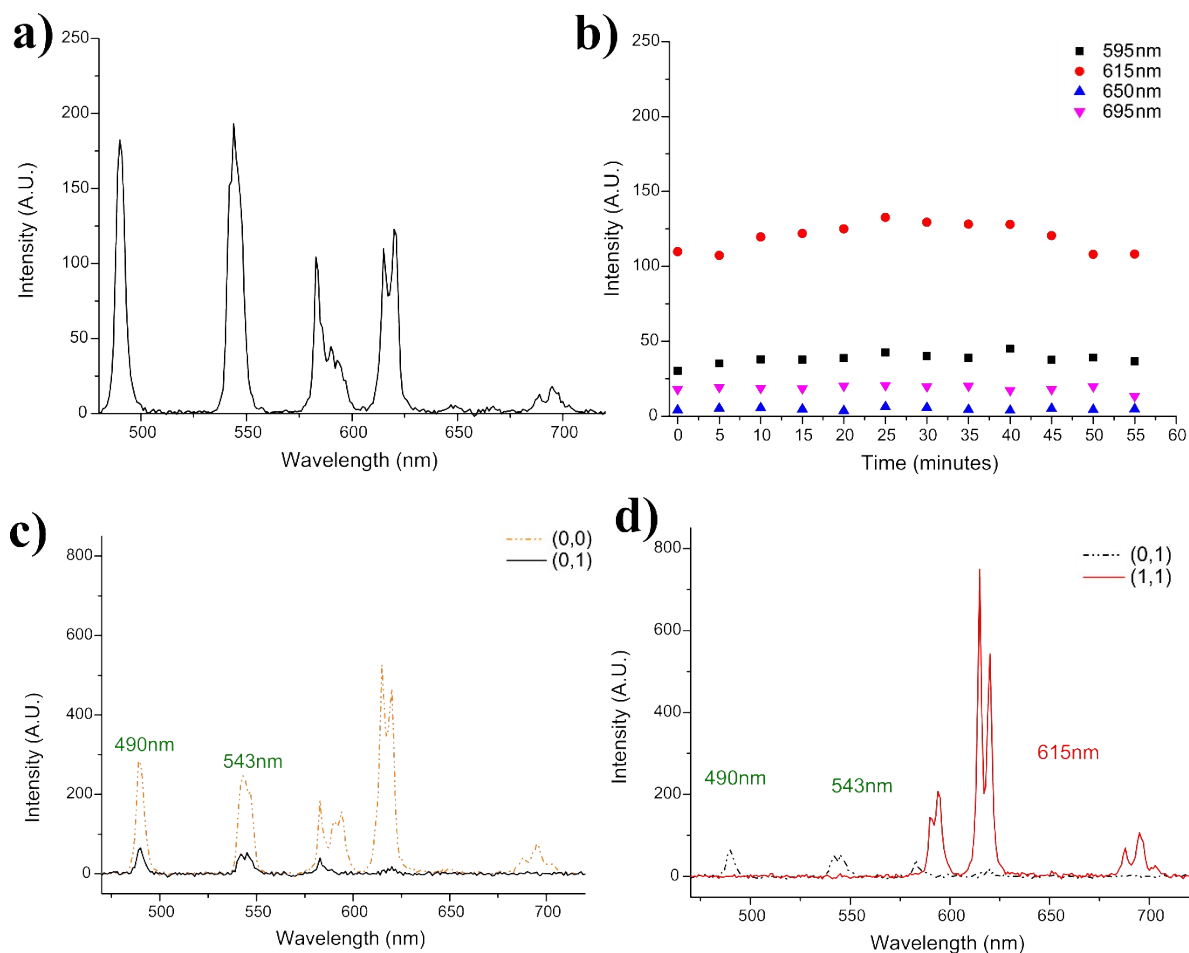
S14 (a) UV-Vis absorbance spectra upon addition of TBAI to a solution of **Tb.2₃** ($c = 1 \times 10^{-5}$ M) in CH_3OH **(b)** Absorbance changes at 300 and 310 nm plotted as a function of TBAI equivalents added



S15 (a) Phosphorescence spectra upon addition of TBAI to a solution of **Tb.2₃** ($c = 1 \times 10^{-5}$ M) in CH₃OH **(b)** Intensity changes in $^5D_4 \rightarrow ^7F_J$ transitions (490, 545, 585, 621 nm) plotted as a function of TBAI equivalents added.



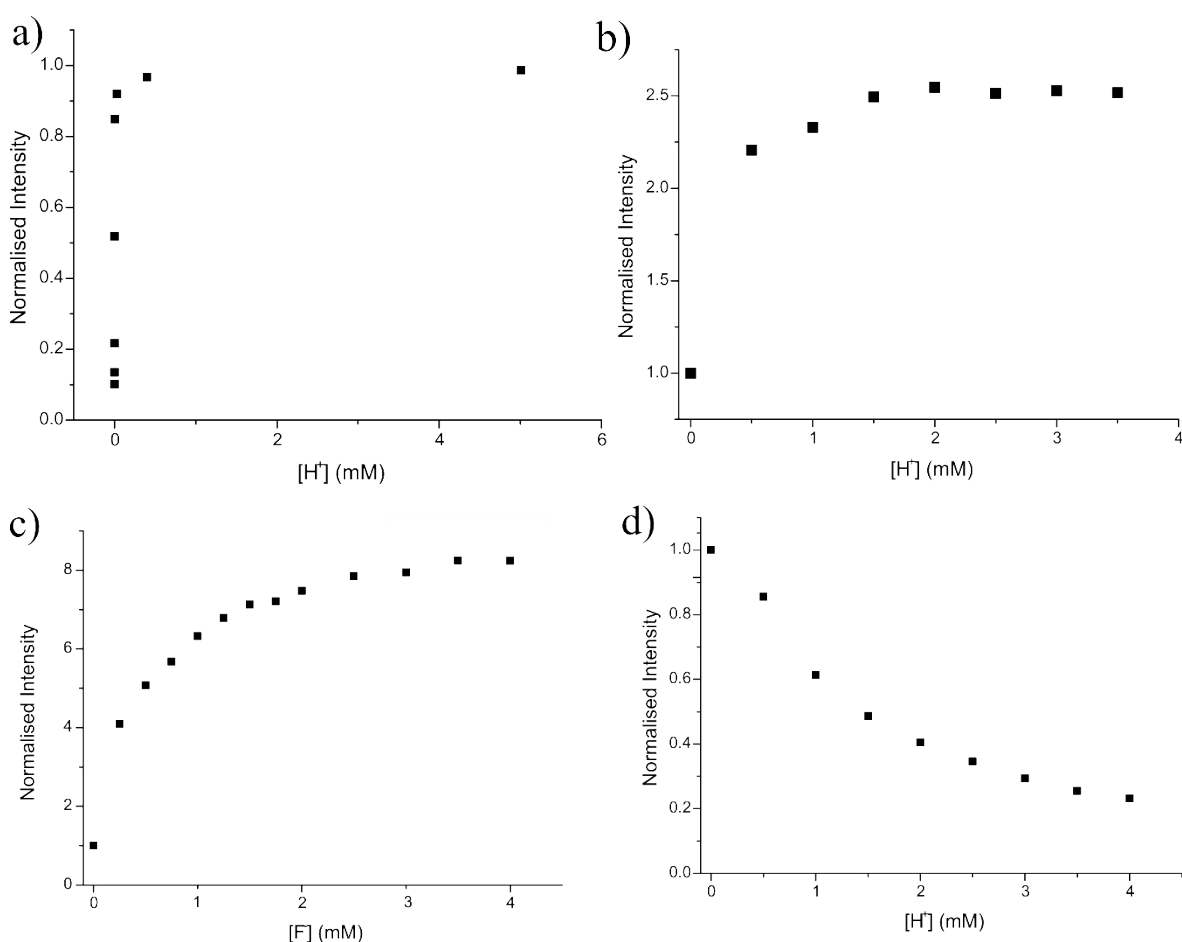
S16 (a) Fluorescence spectra upon addition of TBAI to a solution of **Tb.2₃** ($c = 1 \times 10^{-5}$ M) in CH₃OH **(b)** Intensity changes in the 345 nm band plotted as a function of TBAI equivalents added.



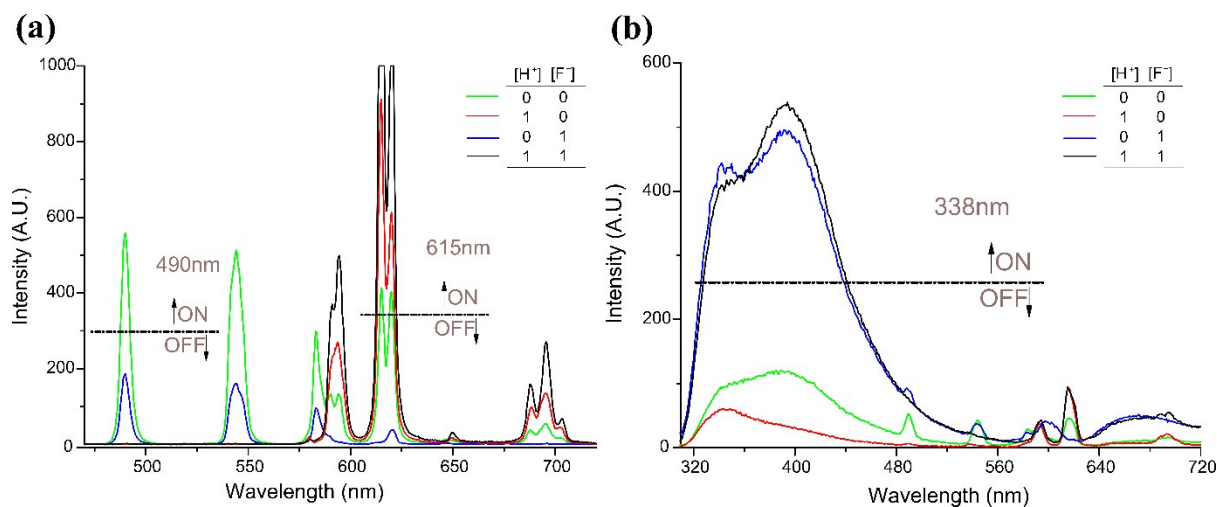
S17 Phosphorescence spectra of gel under excess $\text{Tb}(\text{OTf})_3$ treatment. a) Gel sample reference spectrum; b) Changes in key $\text{Eu}(\text{III})$ centred transitions ($^5\text{D}_0 \rightarrow ^7\text{F}_j$) over time after being exposed to >10-fold excess $\text{Tb}(\text{III})$ as $\text{Tb}(\text{OTf})_3$ in MeOH ; c) Spectra of system emission intensities in phosphorescence upon treatment with F^- [(0,1) state] from neutral [(0,0) state]; d) Spectra of system emission intensities in phosphorescence upon treatment of (0,1) with excess HCl in MeOH [(1,1) state].

Some experimental data is shown in Figure S17 to demonstrate the stability of the system to excess ‘free’ $\text{Tb}(\text{III})$ generated by the dissociation of **Tb.2₃** on exposure to F^- and H^+ . Figure S17a shows a reference spectrum of a gel sample containing both complexes **Eu.1₃** and **Tb.2₃** which was then exposed to excess $\text{Tb}(\text{III})$ as $\text{Tb}(\text{OTf})_3$. Figure S17b shows the changes in emission observed beyond the experimental time period; the intensity of key $\text{Eu}(\text{III})$ transitions were monitored and show no appreciable change over the experiment. The >10-fold excess was substantially more than is ever generated under operating conditions (where ratio of $\text{Tb}:\text{Eu}$ is $\approx 1:2$). From our research on **btp** and **dpa** based systems we see poor $\text{Eu}(\text{III})$ sensitisation from **2** and therefore should substantial scrambling occur we expect that to be reflected by a

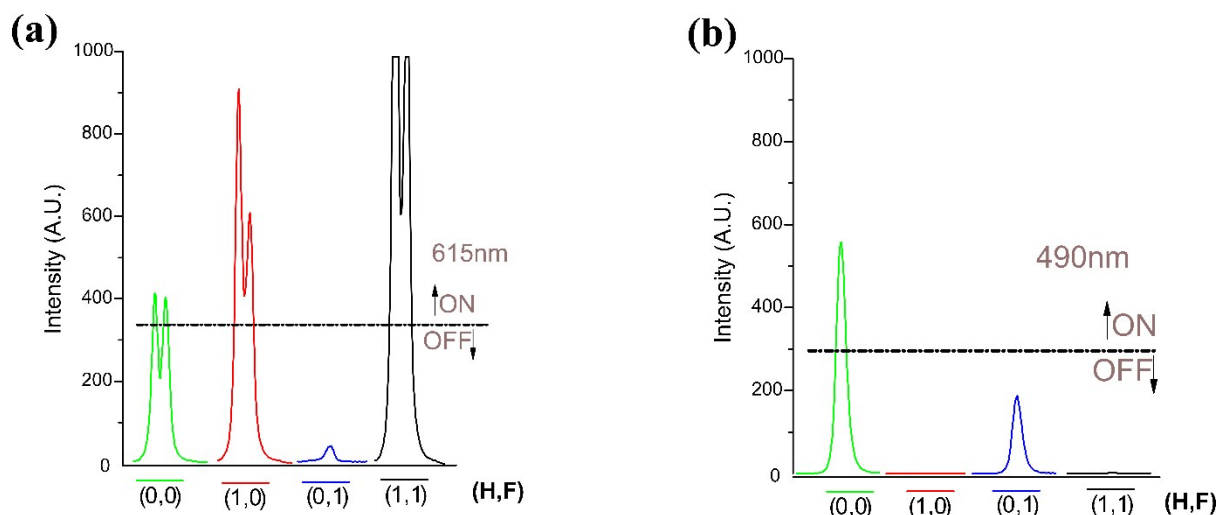
substantial change in Eu(III) emission under neutral conditions. The data in S17b therefore suggests the stability of **Eu.1₃** in the presence of Tb(III) and it can confidently be concluded **Eu.1₃** remains intact within the system. Photo- and thermo- stability of the complexes under operating conditions with repeated irradiation was also demonstrated in these experiments. Figure S17c-d show the experimental spectra from the main article represented to show the change from (0,0) to (0,1) upon fluoridation (Figure S17c) and from (0,1) to (1,1) with F⁻ and H⁺. The “switch-on” from (0,1) to (1,1) in Eu(III) centred emission demonstrated that **Eu.1₃** was stable to excess acid and free Tb(III) and that no substantial scrambling occurred between metal complexes. Again this provided more confidence to the conclusion that **Eu.1₃** remains intact in the presence of dissociating **Tb.2₃**.



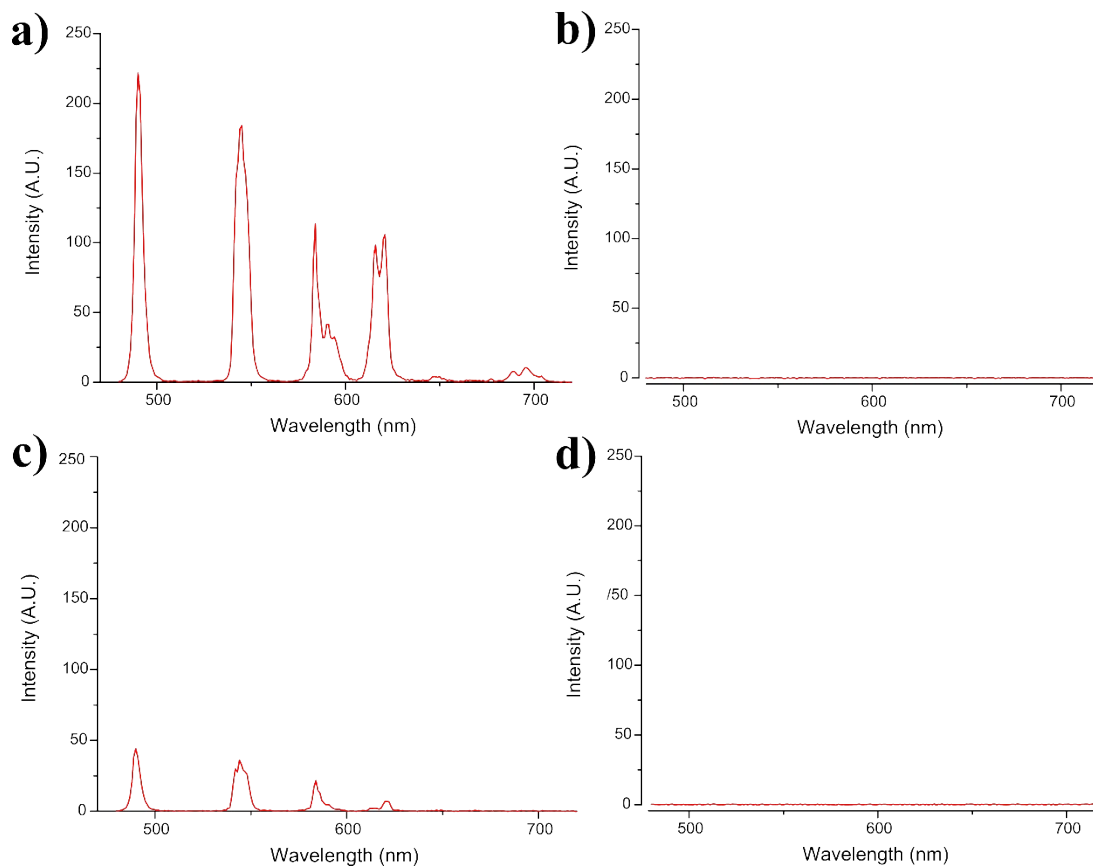
S18 Additional continuous relationships of OUTPUT emissions with INPUT analytes used for guidance of input concentration selection. a) Normalised emission intensity of Eu(III) emission from **Eu.1₃** at 615 nm as a function of [H⁺]; b) Normalised emission intensity of **btp**-centred emission from **Tb.2₃** at 338 nm as a function of [H⁺]; c) Normalised emission intensity of **btp**-centred emission from **Tb.2₃** at 338 nm as a function of [F⁻]; d) Normalised emission intensity of Tb(III) emission from **Tb.2₃** at 490 nm as a function of [H⁺]. Studies carried out in CH₃OH at c = 1 × 10⁻⁵



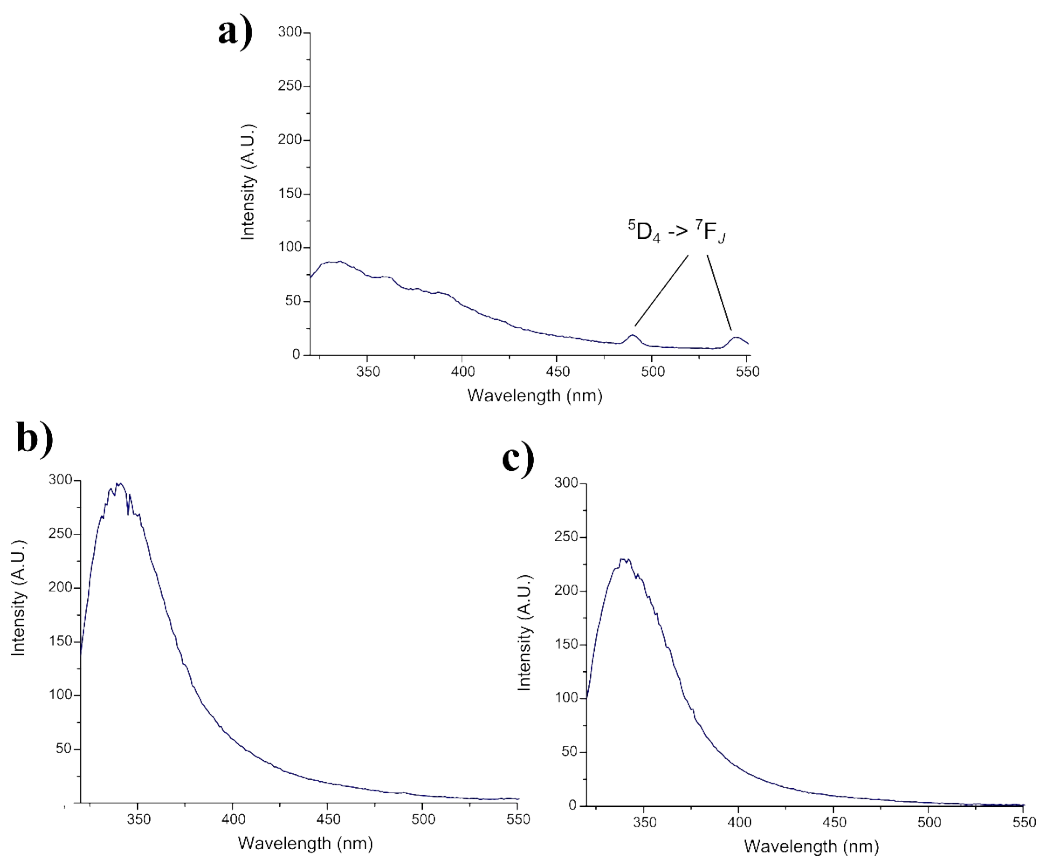
S19 Solution studies in CH_3OH with marked thresholds **(a)** Phosphorescence spectra for (0,0), (0,1), (1,0) and (1,1) input states **(b)** Fluorescence spectra for (0,0), (0,1), (1,0) and (1,1) input states. Thresholds arrive at the same truth table (Figure 2a, main article text). **Eu.1₃**: $c = 2.5 \times 10^{-5}$ M; **Tb.2₃**: $c = 5 \times 10^{-6}$ M recorded in CH_3OH at 24 °C.



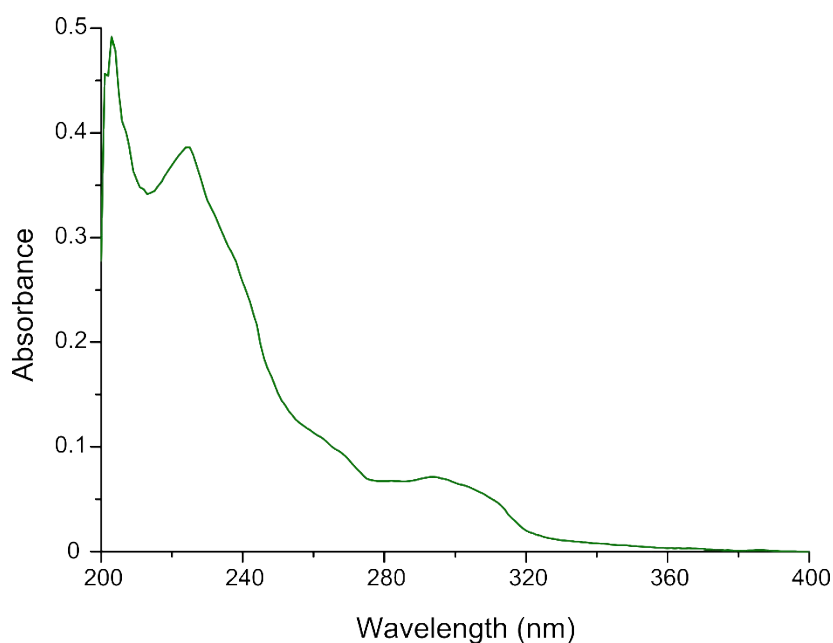
S20 Solution studies in CH_3OH - Split views of phosphorescence signals in (0,0), (0,1), (1,0) and (1,1) input states with thresholds marked for **(a)** Eu(III) $^5\text{D}_0 \rightarrow ^7\text{F}_2$ at 615 nm **(b)** Tb(III) $^5\text{D}_4 \rightarrow ^7\text{F}_0$ at 490 nm. **Eu.1₃**: $c = 2.5 \times 10^{-5}$ M; **Tb.2₃**: $c = 5 \times 10^{-6}$ M recorded at 24 °C.



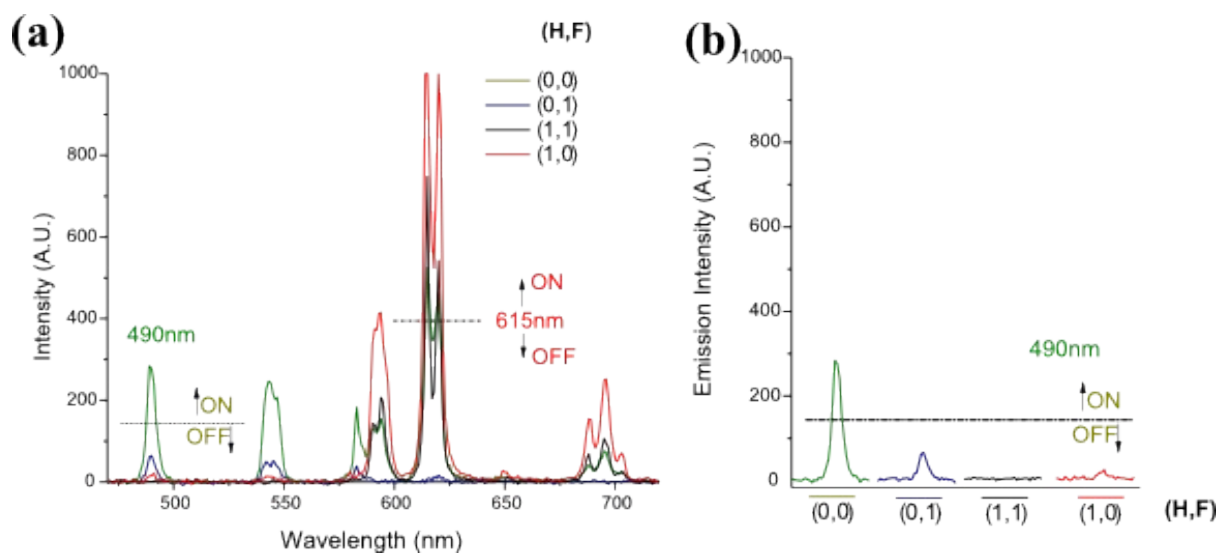
S21 Phosphorescence spectra. a) Full system (gel + supernatant) in (0,0) state (time = 60 minutes); b) Supernatant solution (time = 60 minutes) with gel removed; c) Full system (gel + supernatant) in (0,1) state with F^- (time = 60 minutes); d) Supernatant solution in (0,1) state after F^- treatment (time = 60 minutes) with gel removed



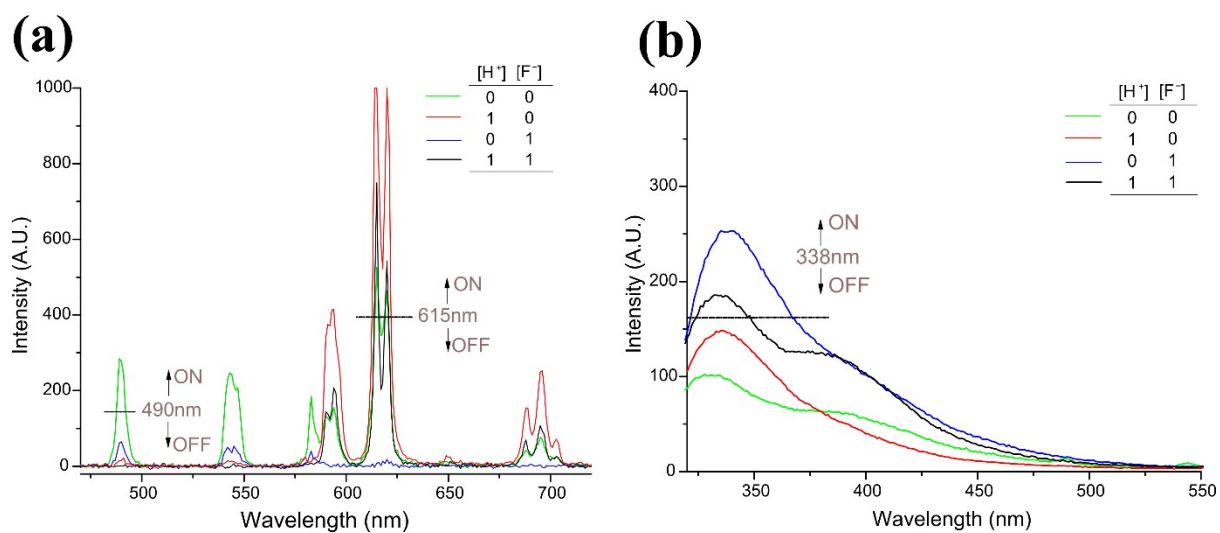
S22 Fluorescence spectra from leeching process. a) Washed gel submerged in CH₃OH in (0,0) state showing Eu.1₃, Tb.2₃ and Tb(III) emissions; b) Full system (gel + supernatant) after F⁻ treatment (time = 60 minutes); c) supernatant solution after F⁻ treatment (time = 60 minutes) with gel removed.



S23 UV-vis absorption spectrum of the supernatant CH₃OH solution after F⁻ treatment (time = 60 minutes) and removal of the organogel. *c.f.* Figures S5 and S8.



S24 (a) Phosphorescence spectra for (0,0), (0,1), (1,0) and (1,1) input states, as seen in main article text; (b) Split view of 490 nm (**Tb.2₃**, metal-centred emission) region for all states with thresholds intensity.



S25 Enlarged gel spectra (Figure 1a and c, main article text) in (a) Phosphorescence; (b) Fluorescence.